Characteristics of Intermittency and ELM Dynamics in the Edge Region of Magnetic Confinement Devices

M. Rajković 1), Tomo-Hiko Watanabe 2), M. Škorić 2)

1) Institute of Nuclear Sciences Vinča, Belgrade, Serbia
2) National Institute for Fusion Science, Gifu, Japan

e-mail: milanr@vin.bg.ac.yu

Abstract. In the approach presented here we combine theoretic aspects and experimental results in order to obtain threefold information on intermittency and edge localized mode (ELM) dynamics using: a) multifractal analysis, b) level-crossing properties of plasma density time series and c) stochastic catastrophy theory (CT). Intermittency properties of the MAST spherical tokamak (L-, H- and dithering H-mode) are considered. Multifractal (MF) analysis suggests that each magnetic confinement device has distinct MF spectral characteristics and that confinement modes (L-, H- and dithering H- modes) exhibit distinct MF spectral features. Also, cascade processes in different tokamak devices are distinct in spite of some universal common features. In the second approach intermittency is studied by considering solely the clustering of level-crossings of turbulent signals and we show that it is related to particles clustering and possibly to accumulation of vorticity. Finally, a reliable estimate of the number of equilibrium states and transitions (bifurcations) between these states is determined. This is important for determining the L-H transition as well as for identifying zonal flow formation. In addition we show that one may infer from experimental data that the ELMs are catastrophic bifurcation events.

1. Introduction

Study of turbulence in magnetic confinement devices represents one of the most important issues in the pursuit of fusion energy production since turbulence hinders confinement, suppresses reactions as it causes particle and energy losses. Control of turbulence requires a thorough knowledge of its dynamics in the core of magnetic confinement devices as well as on the edges beyond the last closed flux surface, in the region known as the scrape-off layer (SOL). A major breakthrough in the confinement improvement occurred by the end of the eighties, when the high confinement (H-mode) was discovered in contrast to the well known L- or low confinement mode [1]. The H- or high confinement mode manifests itself by self-organization of a region just inside the poloidal field separatrix where the transport coefficients are reduced by up to an order of magnitude compared with the L-mode forming a pedestal in the plasma pressure. As a consequence an improvement in the global confinement is usually increased by a factor of two in the case of toroidal devices while it is in the order of ~20% in the case of large helical devices (LHD). The thickness of this barrier-type region is about equal to the ion poloidal gyroradius or the width of an ion banana orbit.

Properties of intermittency both in the case of neutral fluids and plasmas are usually deduced from the analysis of temporal and/or spatial fluctuations of one or several relevant quantities. In the case of neutral incompressible fluids one or all three components of the fluid velocity represent the basic quantity from which all other relevant quantities, such as dissipation, may be derived. In the case of confined plasmas these quantities are usually the ion saturation current, recorded at one or more spatial locations, from which plasma density fluctuations may be inferred and floating potential recorded at different poloidal positions from which radial velocity fluctuations may be determined. In spite of many universal features these two types of turbulence have important differences. Nonlinearites in plasma turbulence are more numerous having different spectral cascade directions in addition to the most important $\boldsymbol{E}\times\boldsymbol{B}$ nonlinearity, leading to more complex fluctuating characteristics. Also, time and space

measurements in plasmas lead to different information on the structure of turbulence. Turbulence in confined plasmas is created and damped at the same spatial location where the measurements are taken so that spatial and temporal informations are interwoven and Taylor's frozen flow hypothesis cannot be applied, a common practice in neutral fluid turbulence studies. For the same reason the inertial range [2], may exist only locally in space or in time, and the extent of this range changes along the temporal scale as well as along space, for example along poloidal direction.

Existence of long-range correlations, noticed in several magnetic confinement devices, suggested that scaling models with a single parameter are appropriate at large temporal scales. However, at small scales, characteristic for intermittency more parameters are needed. As a consequence, a need for multifractal analysis was recognized recently and several studies were devoted to this aspect of plasma turbulence [3, 4, 5, 6, 7]. In Section 2 we present, based on a new approach, main multifractal features of L and H mode turbulence.

Two features of intermittency are its clustering property and the variability in amplitude. Namely, different events cluster together creating uneven density space and time, and events reflected in the highly variable amplitude are dispersed in space and time disproportionately. Much insight into the nature of intermittency may be gained from the study of approximations of turbulent signals which retain only the zero-axis crossings (frequency) information [8, 9]. In Section 3 the clustering properties of these signals are studied based on variance properties of the zero-crossings number in a given time period.

In the studies of strong turbulence [10], the following Langevin equation was obtained as a model for the evolution of turbulence amplitude

$$\frac{dx}{dt} + \Lambda(x)x = \sigma W(t)\,, \tag{1.1}$$

where $\Lambda(x)$ is a deterministic amplification, σ is the diffusion coefficient (assumed constant), $W(t)$ is a Wiener process (i.e. idealized Brownian motion) and x is the amplitude as stochastic variable. In Section 4 we relate this equation to the stochastic catastrophy theory and to the method presented in Section 4 obtaining new insight into the nature of edge localized modes. The conclusion is presented in Section 5.

2. Multifractal Analysis of Turbulent Signals

The ion saturation current fluctuations of reciprocating Langmuir probe installed at the edge of magnetic confinement devices, the quantity used in present analysis, is assumed equivalent to density fluctuations [11]. Recent experimental studies have suggested that intermittency in the SOL of magnetic confinement devices is caused by nonlocal coherent structures denoted as blobs or avaloids [12], which are essentially large-scale structures with high radial velocity, ejected radially towards the wall and encountered intermittently in SOL. These structures lead to a direct loss of matter and energy and hence have a high impact on confinement in contrast to the second type of coherent structures encountered in fusion devices, which represent locally organized fluctuations and which, due to their non radial propagation, contribute less to the loss of confinement. The intermittency properties of the MAST spherical tokamak (L-, H-, and dithering H-mode) are presented here whose MF spectra were generated by consistent use of the measure given by

$$\varepsilon = c\frac{\left(\left|n\frac{dn}{dt}\right| - \left\langle\left|n\frac{dn}{dt}\right|\right\rangle\right)^2}{\left\langle\left(\left|n\frac{dn}{dt}\right| - \left\langle\left|n\frac{dn}{dt}\right|\right\rangle\right)^2\right\rangle} \tag{2.1}$$

where c is a constant. The slope of two-point correlation function using this measure yields intermittency exponent closer to the corresponding value for neutral fluids than the values obtained from other measures. In Fig. 1 the ion-saturation current fluctuations of the 6861 L-, 9031 dithering H- (L/H) and the 5738 H-mode are presented, from left to right respectively. Strong ELM dynamics may be easily noticed in the H-mode while the number of large amplitude bursts in the L/H mode is considerably higher than in the L-mode.

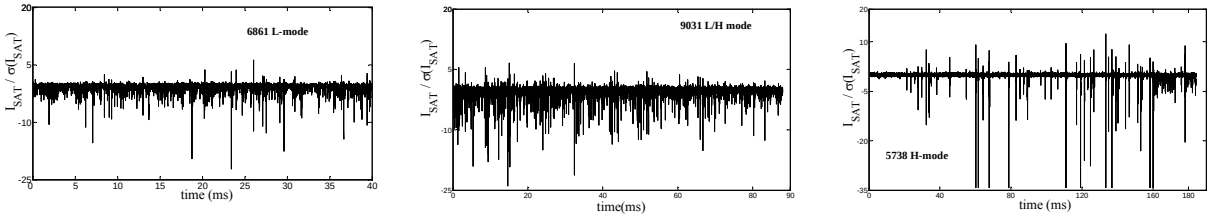

Figure 1. Normalized ion-saturation currents of L-, L/H, and H-mode from left to right respectively.

The large deviation spectra of these time series are presented in Figs. 2 and 3 on different scales, namely for $\Delta t=2^3,\ldots, 2^7$. The Hölder exponent α, shown on the x-axis, quantifies the scaling properties of the process at a given time so that lower values correspond to more abrupt variations. The y-axis represents the probility of occurrence of α in a time series. The most striking feature of these spectra is their departure from a pure bell-shape and concavity and is a good example where Large Deviation Spectra provide more information than Legendre spectra, which are strictly concave although they may be asymmetrical.

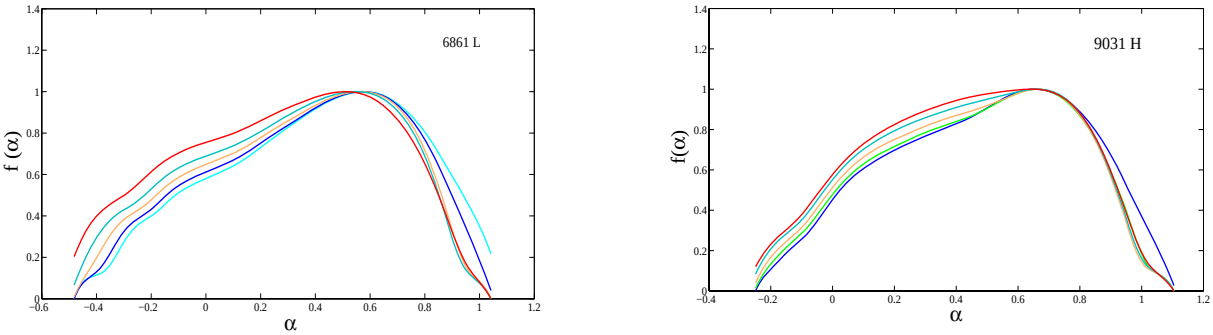

Figure 2. Large Deviation Spectra of the L-mode signal 6861 (left) and the dithering H-mode 9031 (right) of the MAST device for five different scales $\Delta t=2^3,\ldots, 2^7$.

Their shape reflects existence of several multiplicative laws underlying the cascade processes so that there is a lumping of measures whose supports are disjoint. The spectrum of the lumping of two measures resulting in a non concave spectrum is presented in Fig. 4. It is evident that the L-mode has more complex multifractal structure in the sense that there are more α-values at which the irregularity of the spectrum occurs (i.e. more phase changes) than in the case of dithering H-mode. Hence, more measures are lumped and consequently the cascade mechanism and energy transfer is more complex in the case of L-mode. The right-

hand slope of the spectra, both in the case of L- and the L/H- mode, is larger than the left-hand slope, indicating rich variety of strong singularities and their gradual probability of occurrence. The location of the most probable Hölder exponent α_0 for the L-mode is $\alpha_0 \sim 0.6$ and slightly larger $\alpha_0 \sim 0.7$ for the L/H- and H-mode. The width of the spectrum, defined as the $|\alpha_{\max} - \alpha_{\min}|$, is larger in the case of L-mode due to the stronger intermittency effects. Moreover, more irregular instants (degenerate singularities) of fluctuations are present in the L-mode than in the other modes since in the former case the width $|\alpha_{\max} - \alpha_0|$ is larger than for other modes. The spectrum of the H-mode (Fig. 4) clearly reveals the contribution of ELMs (strong singularities of the spectrum) while weak singularities define a concave part of the spectrum which shows no signs of lumping.

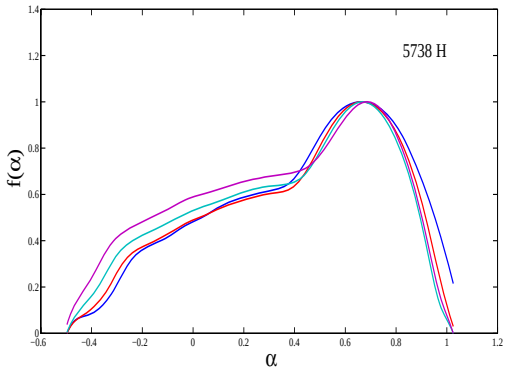

Figure 3. Large Deviation Spectrum of the H-mode 5738 for five different scales.

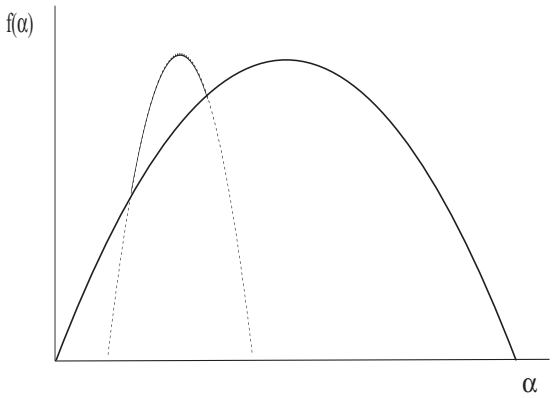

Figure 4. The spectrum of two lumped measures is the maximum of the individual spectra.

3. Clustering Properties of Turbulence Signals

Zero-crossing (or crossing of any particular level of interest) may offer important insight into the underlying process whose temporal variations are studied. The average number of zero-crossings of stationary gaussian process in a specific time interval may be analytically determined and is given by the celebrated Rice formula [13]:

$$N(t) = \lim_{n\to\infty} \int_0^{\tau} \delta(x(t)) \left| \partial x(t) / \partial t \right| dt \tag{3.1}$$

where $\delta(x)$ is the Dirac delta function. Important information on the clustering properties of the signal is however contained in the expression for the variance of the number of zero crossings. The expression for variance again may be derived analytically [14], and is directly proportional to the time interval τ, i.e. $\langle N^2(t) \rangle \sim \tau$. Based on this expression for gaussian process the goal is to contrast clustering properties of turbulent signals with the white gaussian noise. For this purpose a running average within a time interval τ of the number of zero-crossings in τ is evaluated. The fluctuations of the running average are $\delta N(\tau) = N(\tau) - \langle N(\tau) \rangle$, where the brackets denote long-time average, possibly the time of the whole signal. We are interested in the scaling of the variance

$$\left\langle \delta N^2(\tau) \right\rangle^{1/2} = \left[\left\langle N^2(\tau) \right\rangle - \left\langle N(\tau) \right\rangle^2 \right]^{1/2} \sim \tau^{\mu}. \tag{3.2}$$

For a white gaussian noise the clustering exponent is $\mu=1/2$. Since white noise has no clustering, the value of *1/2* indicates lack of clustering. In Fig. 5 we compare the standard deviation of the running density fluctuations for a neutral fluid (left) and the 6861 L-mode (right). Two scaling intervals of the type (2.2) appear dividing the scales of interest into two

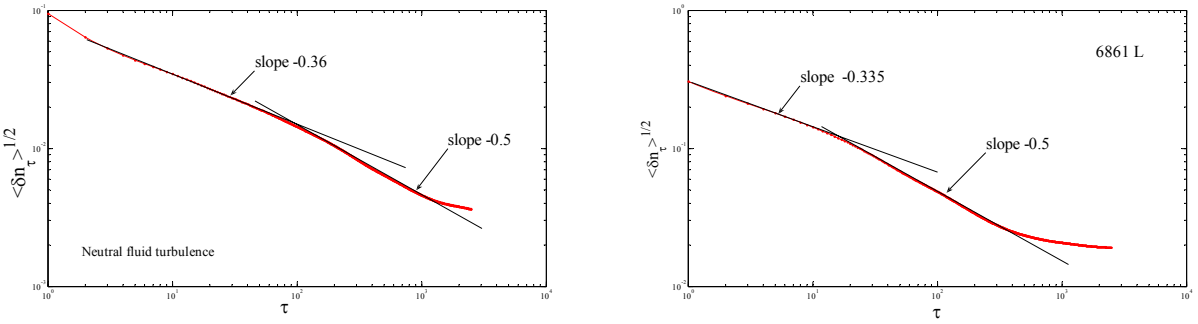

Figure 5. Standard deviation of the running density fluctuations vs. τ for incompressible fluid turbulence (left) and for the 6861 L-mode plasma turbulence (right).

groups which we interpret using the Taylor's frozen flow hypothesis. The scaling interval with exponent ~0.5 suggests that there are no clustering effects for scales larger than the integral scale of the flow. This is an indication that large scales behave as white noise. Small scales with an exponent value less than 1/2 corresponding to the dissipative and inertial range scales show tendency of small scales to cluster. For the L-mode, the clustering exponent is somewhat larger (-0.335 in comparison with -0.36). The extent of large scales is greater and this is due to the large structures of confined plasma turbulence known as blobs or avaloids. These structures do not exhibit clustering since they behave as white noise. Note that the attribute of scales being large or small should be taken in restricted sense, since Taylor's frozen flow hypothesis may not be applicable in the case of confined plasma turbulence. Increased confinement, resulting in the H-mode, may at certain times generate ELMs whose temporal evolution is presented in Fig. 1 (right). In order to investigate the effect of ELMs on clustering we consider the H-mode with ELMs included and with ELMs excluded from the signal. In Fig. 6 the standard deviations of the running density fluctuations for the H-mode

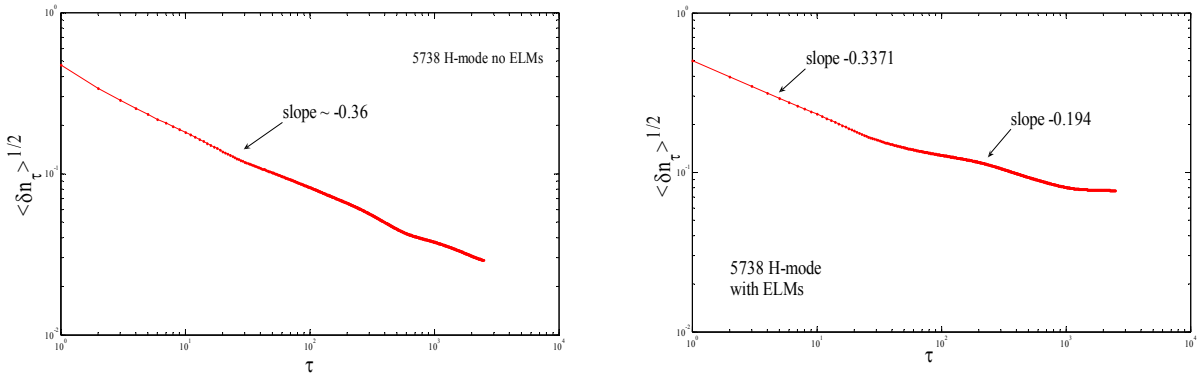

Figure 6. Standard deviation of the running density fluctuations vs τ for the 5738 H-mode with ELMs absent (left) and with ELMs present in the signal.

with ELMs (left) and without (right) are presented. In the absence of ELMs the clustering is evident on all scales with an exponent 0.36 and there are no structures without clustering

effects. Introduction of ELMs causes intense clustering (small slope, exponent ~-0.2), which involves large scales. In comparison with the L-mode which shows no clustering related to large structures as blobs (or avaloids), the large scale structures of H-mode (ELMs) are concentrated sets formed by particles clustering and possibly by accumulation of vorticity. Present analysis offers some interesting conclusions and opens up new areas for understanding plasma turbulence. First, blobs (large scale structures of L-mode) have no clustering properties and are very much different from edge localized modes which are produced by clustering effects. Even small ELMs have different temporal (and most likely) spatial characteristics from blob filaments. Moreover, the overall extent of scales corresponding to blobs surpass the scales corresponding to large scale structures of incompressible fluid turbulence. In the H-mode clustering effects are present on all scales relating this effect to the formation of transport barrier and zonal flows. Since transport is to a large extent suppressed in the H-mode, the value of the clustering exponent can be related to the transport coefficient [15]. Finally, clustering effects may offer new insight about the hierarchy of length scales and their role in the creation of coherent structures

4. Stochastic Catastrophy Theory and the origin of ELMs

The essential feature of Eq. (1.1) is contained in the deterministic term $\Lambda(x)x$ whose form determines stable and unstable equilibria. In the same equation the diffusion function is the square root of the infinitesimal variance function and determines the relative influence of the noise process. We relate this equation to the deterministic CT in which the deterministic amplification represents the gradient of potential function $V(\eta; c_1,...,c_n)$ which incorporates control variables $c_1,...,c_n$ and where η is the deterministic state variable. In general, CT applies to gradient systems that may respond to continuous changes in control variables by discontinuous change from one equilibrium state to another. In particular deterministic CT considers systems whose behavior follows

$$d\eta = -\frac{dV(\eta)}{d\eta}dt\,, \tag{4.1}$$

so that the state of the system changes as a consequence of the potential change. The equilibrium state is determined from the condition $dV(\eta; c_1,...,c_n)/dt=0$. Hence, CT considers systems that move toward an equilibrium state of minimal energy. The link between the potential function of a deterministic system and the stationary probability density function (pdf) of the corresponding stochastic system may be established by considering the stochastic differential equation [16]

$$dx = -\frac{dV(x)}{dx}dt + \sigma(x)dW(t)\,, \tag{4.2}$$

where x is a stochastic variable, $dW(t)$ represents a stochastic Gaussian white noise term (Wiener process) and $\sigma(x)$ is the diffusion function. It is now easy to notice that Eq. (1.1) and Eq. (4.2) are equivalent with $\Lambda(x)x$ corresponding to $-dV(x)/dt$. Since the potential function $V(x)$ and the stationary probability density function (pdf) $F(x)$ convey the same information about the configuration of critical points (i.e. equilibrium points) a stochastic stable equilibrium state may be interpreted as the mode of the pdf. Correspondingly, in stochastic CT stochastic bifurcations are characterized by a change in the number of stochastic equilibrium states or by a change in the number of modes of the stationary pdf. In

deterministic CT the configuration of critical points is invariant under diffeomorphic change of coordinates while in general this is not the case with the stochastic counterpart. However, it was shown in [16] that the product of the pdf *F(x)* and the diffusion function σ, *I(x) = F(x)σ*, is invariant under diffeomorphic transformation of variables. Moreover, it was shown that *I(x)* is a good indicator of the number of equilibrium states. Furthermore, the results presented in [17] have made a connection between *F(x)* and the level crossing probability mentioned in Section 3. Specifically, the probability of crossing a specific level *x* in the next time step Δt is given by

$$P_{\Delta t}(x) = F(x)\sigma(x)\sqrt{2\Delta t/\pi} + O(\Delta t) \tag{4.3}$$

so that the level crossing function $Z(x) = P_{\Delta t}(x)/\sqrt{2\Delta t/\pi}$ approximates the invariant function *I(x)* up to order $\sqrt{\Delta t}$. An estimate of the level crossing function is given by

$$\hat{Z}(x) = \frac{1}{\sqrt{2\Delta t/\pi}} \frac{1}{n-1} \sum_{i=1}^{n-1} \lambda_x(\phi_i, \phi_{i+1}) \tag{4.4}$$

where *n* is the number of observations and $\lambda_x(\phi_i, \phi_{i+1})$ is equal to *1* or *0* depending whether level *x* was crossed by successive observations ϕ_i and ϕ_{i+1} or not respectively.

An important implication of the stochastic catastrophy theory (STC) in the context of confined plasma turbulence is that the information about level crossings of the time series of turbulent plasma density one may obtain a reliable estimate of the number of equilibrium states and transitions (bifurcations) between these states. In this manner a transition from L to H confinement mode may be easily detected and a type of catastrophy involved may be determined. Here we focus on the dynamics of edge localized modes in the H-mode of the MAST device and investigate whether ELMs are related to STC, i.e. whether ELMs are catastrophic bifurcation events. In Fig. 7 (left) we present the estimate of the level crossing function (i.e. *I(x)*) of the 5738 H-mode signal from which the spikes corresponding to ELMs have been removed.

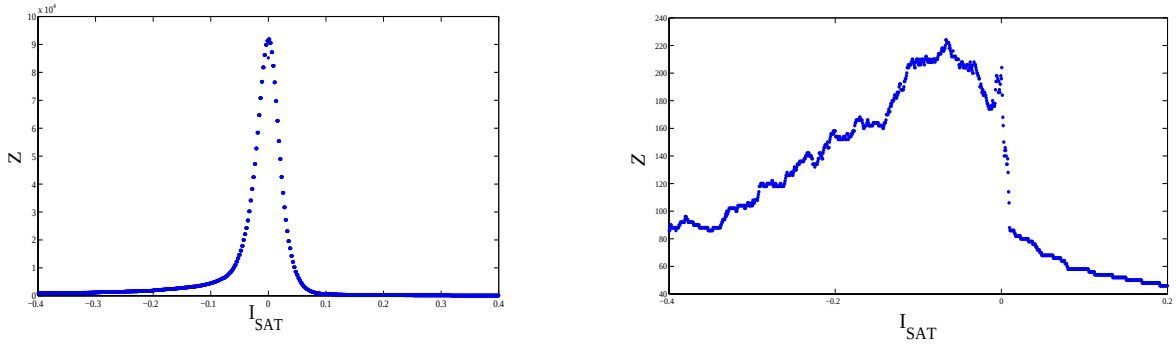

Figure 7. Estimated level crossing function of the H-mode signal without ELM spikes (left) and of the denoised 5738 L-mode including ELMs (right).

Clearly the obtained level crossing function is dominated by the diffusion function $\sigma(x)$ and the level crossing function (i.e. the invariant quantity *I(x)*) is monomodal. The estimated level crossing function of the same signal, however denoised this time, is presented on the right

hand side of Fig. 7. The obtained function shows multimodal features so that it may be inferred that ELMs occur as a result of transitions between different equilibrium states. More importantly, these transitions involve one or more control parameters. Such a scenario rules out self-organized criticality (SOC) as a possible mechanism for ELM generation which assumes that no control parameters are involved.

5. Concluding remarks

Multifractal spectra of plasma turbulent signals based on the Large Deviation formalism reveal important features of turbulence cascading mechanism and offer insight into the processes determining confinement regimes. Level crossing analysis yields clustering properties of turbulence signals and a link with transport properties. Furthermore, this analysis plays an important role in detecting bifurcations of catastrophic type with an important implication that ELMs occur as a result of such processes.

References

[1] The ASDEX team, Nucl. Fusion **29** (1989) 1959.
[2] U. Frisch, Turbulence, the Legacy of A. N. Kolmogorov, Cambridge University Press, Cambridge (1995).
[3] M. Rajković, M. Škorić, K. Sølna and G. Antar, Nucl. Fusion **48** (2008) 024016.
[4] V. P. Budaev, S. Takamura, N. Ohno and S. Masuzaki, Nuclear Fusion **46** (2006) S181-S191.
[5] C. Cloquet, Y. H. Xu, M. Van Schoor, S. Jachmich, M. Vergote and the TEXTOR team, Proceedings of the 33rd EPS Conference on Plasma Physics, Rome, Italy, ECA vol. 301 (2006) P-2.155.
[6] V. Carbone, G. Regnoli, E. Martines and V. Antoni, Phys. Plasmas **7** (2000) 445.
[7] B. Carreras, V.E. Lynch, D.E. Newman, R. Balbin, J. Bleuel, M.A. Pedrosa, M. Endler, B. van Milligen, E. Sánchez and C. Hidalgo, Phys. of Plasmas, **7** (2000) 3278-3287.
[8] K. R. Sreenivasan, A. Bershadskii, J. Stat. Physics **125** (2006) 1145-1157.
[9] A. Bershadskii, J. J. Niemela, A. Praskovsky, K. R. Sreenivasan, Phys. Rev. E **69** (2004) 056314.
[10] -I. Itoh and K. Itoh, J. Phys. Soc. Japan. **68** (1999) 1891.
[11] G. Y. Antar, P. Devynck, X. Garbet and S. C. Luckhardt, Phys. Plasmas **8** (2001) 1612.
[12] G. Y. Antar, S. I. Krasheninnikov, P. Devynck, R. P. Doerner, E. M. Hollmann, J. A.Boedo, S. C. Luckhardt and R. W. Conn, Phys. Rev. Lett. **87** (2001) 065.
[13] S. O. Rice, Bell Syst. Techn. J. **23** (1944) 282-332; **24** (1945) 46-156; these papers are also in Selected Papers on Noise and Stochastic Processes, ed. Nelson Wax, Dover, New York, (1954).
[14] M. R. Leadbetter and J. D. Gryer, Bull. Am. Math. Soc. **71** (1965) 561.
[15] M. Rajković, M. Škorić (in preparation).
[16] L. Cobb, Behav. Sci. **23** (1978) 360-374.
[17] E. Wagenmakers, P. C. M. Molenaar, R. P.P.P. Grasman, P. A. I. Hartelman, H. L. J. Van der Maas, Physuca D **211** (2005) 263.
[18] D. Florens, Stochastic Processes Appl. **39** (1991) 139.